Lab on a Chip

PAPER

View Article Online
View Journal | View Issue

Cite this: *Lab Chip*, 2017, **17**, 936

Tandem emulsification for high-throughput production of double emulsions†

M. L. Eggersdorfer,‡[a] W. Zheng,‡[b] S. Nawar,‡[a] C. Mercandetti,[a] A. Ofner,[a] I. Leibacher,[a] S. Koehler[a] and D. A. Weitz*[ac]

Received 19th December 2016,
Accepted 6th February 2017

DOI: 10.1039/c6lc01553k

rsc.li/loc

Core–shell double emulsions produced using microfluidic methods with controlled structural parameters exhibit great potential in a wide range of applications, but the low production rate of microfluidic methods hinders the exploitation of the capabilities of microfluidics to produce double emulsions with well-defined features. A major obstacle towards the scaled-up production of core–shell double emulsions is the difficulty of achieving robust spatially controlled wettability in integrated microfluidic devices. Here, we use tandem emulsification, a two-step process with microfluidic devices, to scale up the production. With this method, single emulsions are generated in a first device and are re-injected directly into a second device to form uniform double emulsions. We demonstrate the application of tandem emulsification for scalable core–shell emulsion production with both integrated flow focusing and millipede devices and obtain emulsions of which over 90% are single-core monodisperse double emulsion drops. With both mechanisms, the shell thickness can be controlled, so that shells as thin as 3 μm are obtained for emulsions 50 μm in radius.

Introduction

Double emulsions are drops within drops, such as water-in-oil-in-water (WOW) emulsions. Such emulsions have a broad range of applications including encapsulation of active ingredients for pharmaceuticals,[1] food additives[2] and enhanced oil recovery.[3] For many of these applications, it is important to produce double emulsions of core–shell geometry with controlled shell thickness and narrow size distribution. Compared to other commonly used methods like tandem membrane emulsification[4] and phase separation of single emulsions,[5] microfluidic methods offer an exquisite control over drop formation[6] allowing the production of core–shell structures with well-defined features. Double emulsions can be formed in microfluidic devices by various methods, such as through the controlled splitting of a coaxial two-phase jet in glass capillary[7] or in lithography-based microfluidic devices.[8,9] However, for microfluidic methods, the production rate is low. To exploit the superior properties of double emulsions produced by microfluidic devices, it is essential to improve their production throughputs to produce more significant quantities.

Some microfluidic methods are inherently not scalable; for example, glass capillary devices require tapering and manual alignment of individual capillaries, which is a slow process with low reproducibility, since each as-produced device is unique. The only strategy devised so far is to parallelize microfluidic dropmakers to increase the throughput; production rates of single emulsions up to 1000 ml h^{-1} are achieved for flow focusing[10] and 150 ml h^{-1} for millipede (step-emulsification) devices.[11] Lithography-based microfluidic devices are straightforward to parallelize because of their "copy and paste" manner.[12] To parallelize such microfluidic devices, one can integrate many identical dropmakers into a single chip and connect the inlets for the dispersed and continuous phases, as well as the outlet for the as-produced emulsions *via* shared distribution and collection channels.[13–15] As such, through careful design, it is possible to have many dropmakers operating in parallel without hydrodynamic interactions between individual dropmakers, thus allowing scalable production of uniform emulsions. However, to form double emulsions, it is critical for the microfluidic device to have spatially controlled wettability: the first junction should wet the shell phase while the second junction should wet the

[a] *School of Engineering and Applied Sciences, Harvard University, Cambridge, Massachusetts 02138, USA. E-mail: weitz@seas.harvard.edu*
[b] *Department of Chemistry and Chemical Biology, Harvard University, Cambridge, Massachusetts 02138, USA*
[c] *Department of Physics, Harvard University, Cambridge, Massachusetts 02138, USA*

† Electronic supplementary information (ESI) available: High-speed camera movies showing the generation of double emulsions with a single core (S1) and a double core (S2) in the millipede device and the effect of the outer phase flow rate on single core double emulsion formation in the flow focusing device (S3). See DOI: 10.1039/c6lc01553k

‡ These authors contributed equally to this work.

outer phase. Although this can be accomplished for single nozzle devices through methods such as flow confinement, these methods cannot be reproducibly applied to parallelized devices, since for successful surface modification, all parallelized junctions should be properly treated. Thus, given the difficulty of achieving spatially controlled wettability in parallel devices, it is challenging to robustly scale-up production rates of double emulsions. This problem can be circumvented for example by producing only oil-in-oil-in-water (OOW) double emulsions[16] as this does not require spatially controlled wettability. Another method is to use a non-planar design which has a change in height at the location of drop break-up.[17] However, for these methods, flow rates of the continuous phase or material selection are critically limited. As such, to robustly scale up the production of core–shell double emulsions, it is critical to devise an approach to overcome the limitations posed by the difficulty of obtaining spatially segregated wettability in parallelized dropmakers.

In this paper, we describe an approach for the mass production of water-in-oil-in-water core–shell double emulsions that solves the problem of robustly parallelizing microfluidic devices through the use of tandem emulsification to achieve spatially segregated wettability. In tandem emulsification, we directly reinject emulsions made from the first device into the second one to produce double emulsions,[18–20] with the surface of each device appropriately functionalized before the devices are connected. As the modification of a whole device is facile and allows uniformity throughout all channels, with tandem emulsification, many dropmakers can be parallelized into one set of devices, thus vastly increasing the production rate of single-core double emulsions. This method can be applied to both flow focusing devices[21] and millipede (step emulsification) devices,[22] and over 90% of the emulsions obtained by both methods are single-core monodisperse double emulsion drops. Tandem emulsification maintains exquisite control over drop formation for double emulsions with both mechanisms, the shell thickness of single-core double emulsions can be controlled and volume fractions as high as 66% can be obtained. The double emulsion volume fraction is defined as the volume of double emulsions produced divided by the total volume of all dispersed and continuous phases used. Our methods provide a scalable, robust approach for the production of double emulsions with controlled parameters.

Results & discussion

We demonstrate the use of tandem emulsification by both flow focusing and millipede polydimethylsiloxane (PDMS) microfluidic devices fabricated by soft lithography. A set of tandem emulsification devices consists of two devices whose surfaces are modified separately before connecting them. Each device has two inlets and one outlet: the outlet of the first device is directly connected to the inlet for the dispersed phase in the second device, so that in total, only three pumps are required for the tandem emulsification setup, as shown by the scheme in Fig. 1a–f.

We first consider a set of flow-focusing devices as presented in Fig. 1a: in the first flow focusing device, we form monodisperse water-in-oil (WO) single emulsions with a coefficient of variation (CV) of drop diameter <0.05 as magnified in Fig. 1b. We operate the first device in a dripping regime to achieve better control over emulsion formation because in this range, the drop diameter varies steadily with flow rates thus it is easier to control the drop size, as shown in Fig. S1.† The single emulsions formed in the first device are continuously transferred to the second device, where water-in-oil drops are encapsulated by the continuous aqueous phase resulting in WOW double emulsions; the temporal evolution of this process is shown in Fig. 1c. The same dropmaker design is used for the first and second devices, however, the surface functionalization changes due to the necessary contact angle condition for drop formation. The outer phase needs to have a lower contact angle than the inner phase at the location in the device of de-wetting and drop break-up. For example, to generate WOW drops, the channels of the first device are hydrophobic and oil wets the walls for WO drop formation while the second device is rendered hydrophilic and the continuous water phase wets the walls to generate WOW drops.

A critical parameter is the ability to control the core number of the drops produced. The core number is related to the as-produced double emulsion core and shell sizes, which is determined by the flow rate ratio of the inner and middle phases. In flow focusing devices, the drop diameter highly depends on the flow rates of the dispersed and continuous phases because the break-up is governed by two competing forces: the viscous shear force of the continuous phase stretching the liquid thread downstream and the surface tension holding it together.[23] Thus, we find that as the ratio of the inner phase flow rate to the middle phase flow rate increases in the first device, we obtain larger drops, as shown in Fig. S2a.†

We study the core number and flow rate relationship with a set of identical flow focusing devices. A flow rate of the inner and middle phase of $q_i = q_m = 800$ μl h^{-1} was used while we change the outer phase flow rate q_o. The fraction of single-core double emulsions is high when the flow rate is between $800 < q_o < 1200$ μl h^{-1}. Multi-core double emulsions are generated for $q_o < 800$ μl h^{-1}. In this case, the outer phase flow is too weak to trigger the drop break-up on time to encapsulate only a single core. However, in the other extreme for $q_o > 1200$ μl h^{-1}, only every other drop formed in the second device contains a drop, since the drop break-up frequency is higher than the frequency at which the drops reach the tip of the nozzle. At an outer phase flow rate of 1200 μl h^{-1}, we obtain a 95% yield of WOW single core double emulsions. These results are shown in Fig. 2a. We also fix the flow rate of the outer phase and vary the ratio of inner to middle phase flow rates. At a flow rate ratio of inner to middle phases around 1, we obtain the highest portion of single-core double emulsions for most of the outer phase flow rates tested as shown in Fig. S2b.†

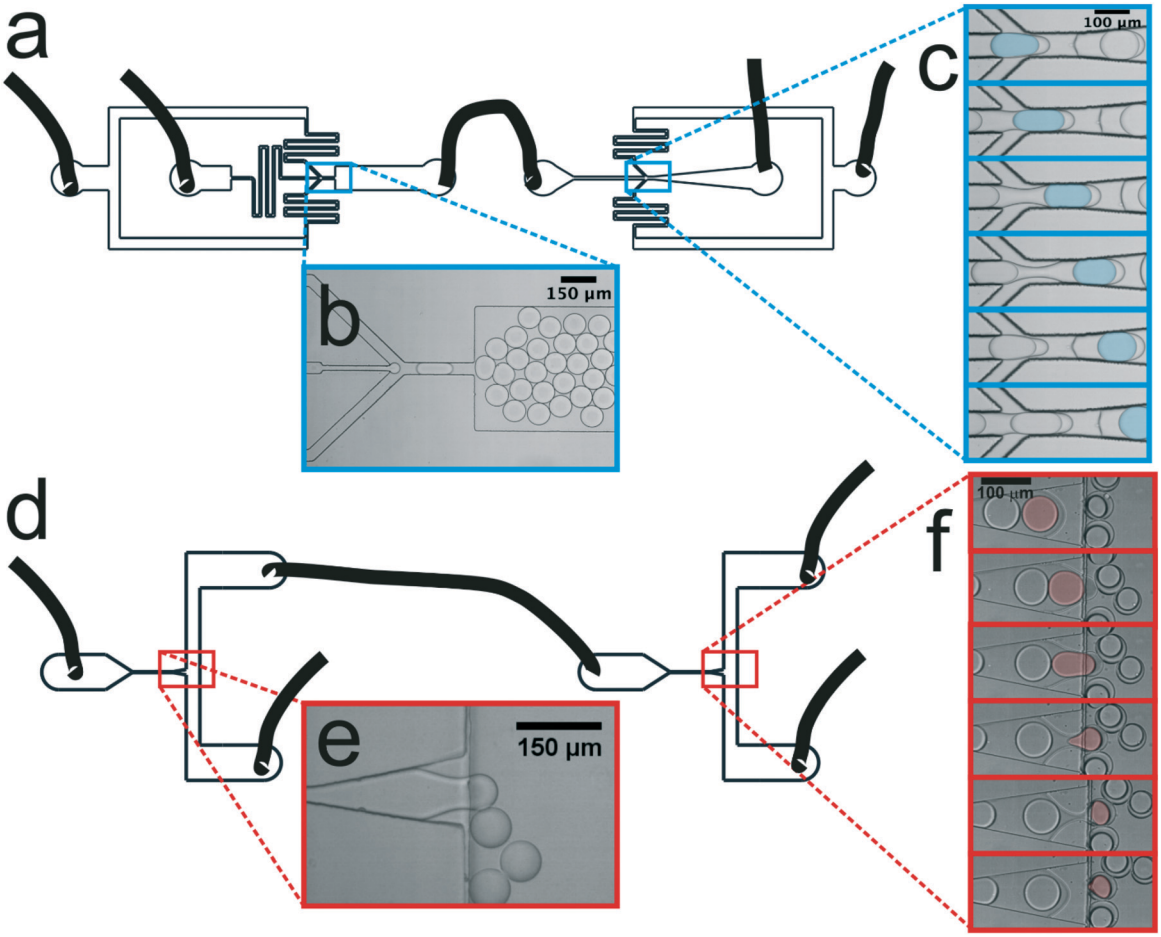

Fig. 1 Sketch of the tandem operation of two a) flow focusing and d) millipede (step-emulsification) devices in series with a magnification of the droplet generation at the first junctions in b) and e) and evolution of the encapsulation of a droplet by c) flow focusing highlighted in blue and f) step emulsification highlighted in red.

Another important parameter of the single-core double emulsions is the average shell thickness, x, which is half of the difference between the inner and outer diameters. We change the shell thickness of the core–shell double emulsions produced by changing the channel height of the 1st flow focusing device while keeping the 2nd device height constant. By increasing the channel height of the first device, H_1, from 20 μm to 50 μm and 100 μm, the inner drop diameter d_i and double emulsion diameter d_o both change, and the shell thickness of the resulting double emulsions decreases from 22 μm to 3 μm, corresponding to a relative shell thickness, x/r, decrease from 60% to 5%, with r being the droplet radius. This is shown in Fig. 3a. One interesting thing here is that increasing the channel height from 50 μm to 100 μm does not increase the inner diameter in the double emulsions. This is because the large drops formed in the first device are split into several smaller drops during re-encapsulation to form double emulsions in the second device, similar to the operation of ultra-thin shell formation in glass-capillary[24] or non-planar lithography-based devices.[25] The double-emulsion drop diameter is set by the outer water flow rate and is chosen to maximize the fraction of single-core double emulsions. For the 20 μm height device, the maximum fraction of single core drops achieved is only about 40%, while it is over 95% for the 50 μm and 100 μm height devices. The theoretical flow rate ratio by mass balance to obtain single core double emulsions with d_o = 70 μm and d_i = 30 μm is $q_m = 17q_i$. Nevertheless, even operating close to the

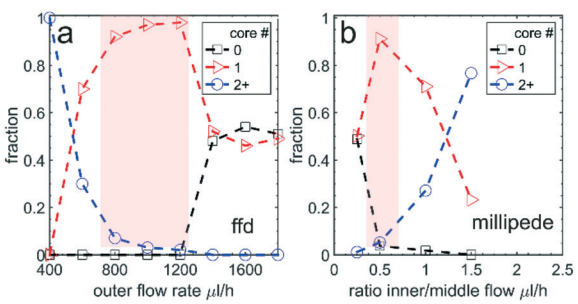

Fig. 2 The fraction of no-, single- and two-plus-core double emulsions as a function of a) the outer flow rate for the flow focusing device and b) the ratio of inner to middle flow rates for the millipede device. The ideal working range with the highest fraction of single-core double emulsions is highlighted. The broken lines are drawn as guides to the eye.

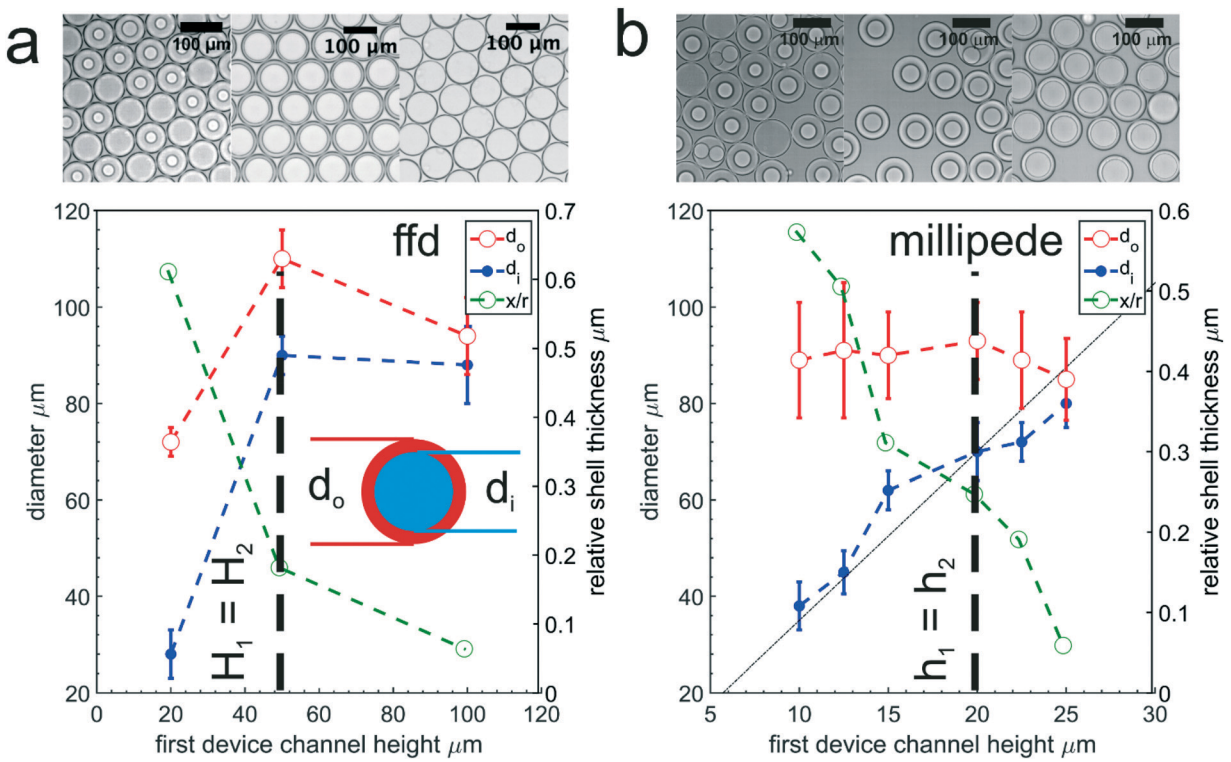

Fig. 3 Shell thickness, *x*, control with flow focusing and millipede devices. a) Control of the relative shell thickness, *x*/*r*, by changing the channel height H_1 of the flow focusing dropletmaker in the first device and keeping the channel height H_2 in the second device constant. The shell thickness depends on the diameter of the inner droplet d_i and outer droplet d_o. Top images show double emulsions produced with different core sizes with tandem flow focusing devices. b) Control of the shell thickness by changing the height h_1 of the high aspect ratio nozzle in the first device and keeping the channel height h_2 in the second device constant. Increasing the nozzle height results in larger d_i while d_o remains constant, hence decreasing the shell thickness. The broken lines are drawn as guides to the eye. Top images show double emulsions produced with different core sizes with tandem millipede devices. The black dashed vertical line highlights the condition with equal channel heights in the first and second devices.

theoretically ideal flow rate ratio results in a large fraction of single emulsions at ~40% and multi-core double emulsions at ~20%. This occurs because it is very challenging to control the re-injecting frequency and spacing between drops if the flow rate ratio of $q_m \gg q_i$, and as such, the encapsulation statistics under such dilute conditions converges to a Poisson distribution.

We also applied tandem emulsification with millipede devices as shown in Fig. 1d, similar to the setups applied to flow focusing tandem emulsification. Uniform single emulsions are produced in the first millipede device in the dripping regime, as shown in Fig. 1e, and are re-injected into the second millipede device with different surface functionalization. The temporal evolution of the encapsulation of a water-in-oil drop into the continuous water phase resulting in WOW emulsions is shown in Fig. 1f.

In millipede devices, a triangular reservoir is added to the end of each nozzle; this reservoir slows down the fluid flow, and establishes quasi-static conditions, so the drop size in the dripping regime depends on the device geometry and properties of continuous and dispersed phases rather than flow rates of inner or middle phases.[26–28] As a result, the drop diameter of double emulsions and the core size of single-core double emulsions are determined by the channel height of the second and first millipede devices, respectively. Thus, with a specific set of millipede tandem emulsification devices, to maximize the percentage of single-core double emulsion drops in the produced emulsions, the ideal flow rate ratio of the inner to middle phase flow rates is equal to the volume ratio between the core and shell materials of the as-produced single-core double emulsions. With two millipede devices having the same channel height h = 20 μm, the as-produced WOW single-core double emulsions are about 100 μm in diameter with a core diameter around 70 μm, which corresponds to a 1 : 2 core-to-shell material ratio. We vary the ratio of q_i and q_m to optimize the fraction of single-core double emulsions obtained. The maximum percentage of single-core double emulsions is achieved at a ratio of $q_i : q_m$ = 1 : 2 which is in good accord with the calculated value. At this ratio, over 90% of the formed drops are single-core double emulsions. Multi-core double emulsions are attained at a ratio of $q_i : q_m \geq 1$. For the ratio of $q_i : q_m < 0.5$, the frequency of the re-injected water drops is too low compared to the pinch-off frequency in the second millipede device. Consequently, every other drop is an oil-in-water drop. These results are shown in Fig. 2b. The formation of single- and double-core double emulsions by step-

emulsification in a controlled manner is shown in videos S1 and S2.†

Shell thickness control in tandem millipede devices is straightforward as we can simply change the device height to change the core and double emulsion diameters. We demonstrate shell thickness control in tandem millipede devices by keeping the channel height of the second device the same while changing the channel height of the first device from 10 μm to 25 μm. d_o remains nearly constant around 90 μm, while d_i matches the empirical relation reasonably well. As a result, the shell thickness varies from 26 μm to 3 μm, corresponding to a decrease in the relative shell thickness from 0.58 to 0.07, as shown in Fig. 3b.

We parallelize both flow focusing and millipede dropmakers in a 2D array to scale up their production levels. Only a single inlet is required for each of the inner, middle and outer phases to feed the dropmakers, and the product is collected from a single outlet. The dimensions of the dropmakers used to generate WO drops in the first device and the dropmakers used to generate WOW double emulsions in the second device are identical. The inner phase in the first device or single emulsions in the second device enter through the inlet and are evenly distributed by bifurcations to the individual nozzles in the flow-focusing devices. Thus, the number of nozzles is by design always a power of two. Here, the bifurcations are crucial, since for flow-focusing, drop breakup is governed by the shear exerted by the continuous phase on the dispersed phase, and as such, a uniform distribution of the dispersed and continuous phases among dropmakers in the parallelized device is necessary for achieving uniform production rates and sizes across all nozzles. The distribution channels of the outer phase are a mirror image of that of the inner phase, but with one additional bifurcation to pinch-off the inner phase flow symmetrically from two sides. We also add an additional layer which connects all outlets of the first layer to one large channel to form a single outlet.[13] Such a collection or distribution channel[13,29,30] is an elegant way to reduce the number of connections and pumps, although it requires through-holes in the first layer and an additional bonding step. This design is shown in Fig. 4a.

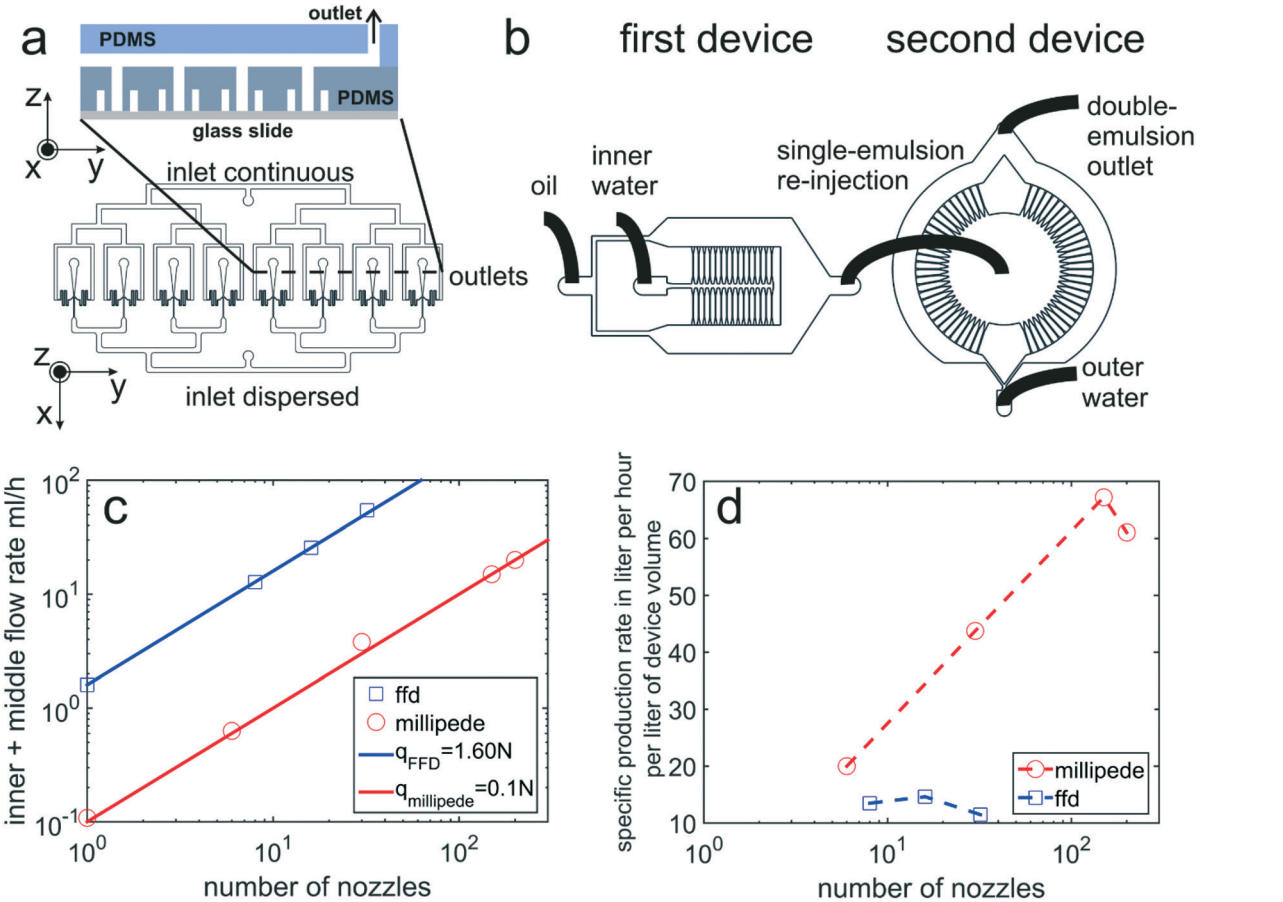

Fig. 4 Scale-up production of double emulsions. a) Flow focusing devices are copied and pasted in a row with a single feed for the continuous and dispersed phases. An additional PDMS layer is bonded on top of the device to connect all outlets by one channel to collect all droplets and lead them through a single tube to a vial. b) Step-emulsification nozzles are arranged along a straight distribution channel in the first parallelized device. In the re-injection device, the nozzles are radially distributed around the inlet to achieve a homogenous encapsulation. c) Flow focusing devices (FFD) have an order of magnitude higher flow-rate per nozzle than millipede devices. The maximum throughput scales linearly with the nozzle number for both methods. d) However, the throughput per device volume or specific throughput increases faster for millipede than flow focusing as the millipede devices can be arranged more economically. The broken lines are drawn as guides to the eye.

In contrast to the parallelized flow-focusing devices, in the millipede devices, there is less need for even distribution of the dispersed and continuous phases to each channel, and as such, we circumvent the need to use bifurcations to evenly feed each dropmaker. Thus, millipede dropmakers can be more closely packed. A linear arrangement of dropmakers is most economical in terms of space and commonly applied for single emulsion generation.[31] However, if we re-inject single emulsion drops into a millipede device with a linear arrangement, the re-injected drops accumulate towards the end of the linear inner-phase distribution channel. The volume fraction of single-emulsion drops is between 10–20% close to the device inlet and increases to almost 80% for the nozzles farthest away from the inlet as shown in Fig. S3a and b of the ESI.† Thus, with a linear configuration, the nozzles closer to the inlet produce a high fraction of oil drops with no core while the nozzles farther away from the inlet produce multi-core double emulsions. Thus, to achieve a homogeneous distribution among dropmakers compared to a linear device, we arrange the dropmakers in a circular device so that they are radially distributed around the inlet,[28,32] as shown in Fig. 4b. In circular devices, drops are re-injected with nearly the same rate into each dropmaker, as shown in Fig. S3a and c of the ESI.†

We also investigate the production rate, which is the sum of the inner and middle phase flow rates, for the parallelized devices. The production rates scale almost linearly with the number of nozzles for the investigated range for both parallelized flow focusing and millipede devices, as shown by the blue squares and red circles for parallelized flow focusing and millipede devices, respectively, in Fig. 4c. The production rates decrease with increasing viscosity of the inner or middle phases in the flow focusing[33] and millipede devices.[34] The lower throughput can be partially compensated in the flow focusing devices by increasing the continuous phase viscosity.[33] In contrast, in the millipede devices, the throughput still decreases with increasing viscosity of the continuous phase.[34] Nevertheless, we expect the production rate to increase further by increasing the number of nozzles in a device, for example, by 3D parallelization using several layers of flow focusing[10,30] or millipede devices. Another important figure of merit for scaled-up production of double emulsions is the specific production rate, which is the production rate per volume of the device, as it is key for assessing the performance of parallelized dropmakers. For millipede devices, initially, as the number of nozzles increases, the specific production rate increases almost linearly. This occurs because common regions such as inlets, outlets, distribution channels and the reinjection reservoir dominate the device volume when there are not many nozzles, and as such, adding additional nozzles only slightly increases the total device volume. By contrast, for the parallel flow focusing devices, the specific production rate does not change much as we pack more nozzles, because the total device volumes of the parallelized flow focusing devices scale almost linearly with the number of nozzles. This occurs because the incorporation of additional nozzles in the parallel flow focusing devices requires addition of bifurcating channels for the distribution of the dispersed and continuous phases to each nozzle. Despite the low production rate per nozzle, the millipede devices have a higher specific production rate than the flow focusing devices for the range investigated due to their denser packing of nozzles. The specific production rate, measured as double emulsion production rate in liters per hour per liter of device volume, as a function of nozzle number is shown in Fig. 4d.

Experimental

The microfluidic devices are fabricated with PDMS (Dow Corning Sylgard 184, MI) using conventional soft lithography with a negative photoresist (SU8, Microchem, MA).[12] We apply two layers of the photoresist and two UV exposure steps to produce a step in channel height for millipede devices.[35] The thickness of the second layer is five to ten times the height of the first layer. The transparency mask for the second exposure is aligned with the first layer using a mask aligner (ABM, CA). The PDMS channels are closed by bonding the PDMS to glass using oxygen plasma (Plasma Etch, PE 50-HF, NV) for 12 s at 30 W. The surface of the first device is rendered hydrophobic by flushing all channels with a solution of 2 vol% trichloro(1*H*,1*H*,2*H*,2*H*-perfluorooctyl)silane (Sigma-Aldrich, MO) dissolved in fluorinated oil (Novec 7500, 3M, MN). The second device is immersed in DI water right after plasma bonding to conserve its hydrophilic surface properties and used within a few hours after bonding. For parallel flow-focusing devices, an additional layer containing the collection channel is bonded to the PDMS layer containing dropmakers using oxygen plasma for 30 s at 80 W.

The liquid phases are injected into the device through polyethylene tubing (PE/5, Scientific Commodities Inc., AZ) using pumps (Harvard Apparatus, MA). We use DI water for the inner phase with a viscosity of η = 0.89 mPa s, fluorinated oil (Novec 7500, 3M, MN) with 1 wt% surfactant (PEGylated Krytox, RAN Biotechnologies, MA) and η = 1.41 mPa s for the middle phase, and DI water with 1 vol% Triton X-100 (Sigma-Aldrich, MO) with η = 1.01 mPa s for the outer phase. The viscosities are measured with a rheometer using a double gap concentric cylinder (MCR 501, Anton Paar, Austria). Images and movies are acquired with an inverted microscope (Leica, Germany) using 5× and 10× objectives and a high speed camera (Phantom V9, Vision Research, NJ). The drop sizes are analyzed with ImageJ software. We measure the interfacial tension using the pendant drop method on a home built tensiometer.

Conclusions

We use tandem emulsification to achieve robustly segregated wettability in parallelized microfluidic devices for the scaled-up production of single-core WOW double emulsions. We demonstrate tandem emulsification in parallelized flow focusing and millipede devices for the production of double emulsions with controlled shell thicknesses. We achieve

production rates of about 60 mL h^{-1} for 32 parallelized flow focusing devices which corresponds to a frequency of 630 droplets per second and nozzle, while for tandem millipede devices, we achieve production rates of 20 mL h^{-1} using a device with 200 parallelized nozzles which is equal to a frequency of 80 droplets per second and nozzle. The production rates obtained are comparable to those previously reported for WOW double emulsions produced using parallelized dropmakers. However, tandem emulsification allows easy device fabrication and convenient segregated surface modification thus double emulsions with a high volume fraction can be produced in a well-controlled manner. Additionally, this method is applicable to a wide range of core and shell materials, and as such can be used to scalably produce a diverse array of microcapsules. While we have demonstrated the scaled-up production of WOW double emulsions using tandem emulsification, this method can easily be applied to produce OWO double emulsions by reversing the wettabilities of the first and second devices. Furthermore, we can also produce higher order emulsions, such as triple emulsions, by re-injecting the as-produced WOW or OWO double emulsions into a third device for re-encapsulation. Our approach provides a general route for the scaled-up production of complex emulsions with well-controlled structural parameters.

Acknowledgements

M.E. received funding from the Swiss National Science Foundation (grant no. P2EZP2-148643). This work was performed in part at the Center for Nanoscale Systems (CNS), a member of the National Nanotechnology Infrastructure Network (NNIN), which is supported by the National Science Foundation under NSF award no. ECS-0335765. The CNS is part of Harvard University. We thank Liangliang Qu for her support with the viscosity measurements.

References

1 T. G. Park, H. Yong Lee and Y. Sung Nam, *J. Controlled Release*, 1998, **55**, 181–191.
2 R. Wegmueller, M. Zimmermann, V. G. Buehr, E. J. Windhab and R. F. Hurrell, *J. Food Sci.*, 2006, **71**, 181–187.
3 J. Sheng, *Chemical Enhanced Oil Recovery: Theory and Practice*, Gulf Professional Publishing, 2010.
4 K. Akamatsu, W. Chen, Y. Suzuki, T. Ito, A. Nakao, T. Sugawara, R. Kikuchi and S. I. Nakao, *Langmuir*, 2010, **26**, 14854–14860.
5 P. J. Dowding, R. Atkin, B. Vincent and P. Bouillot, *Langmuir*, 2004, **20**, 11374–11379.
6 S.-Y. Teh, R. Lin, L.-H. Hung and A. P. Lee, *Lab Chip*, 2008, **8**, 198–220.
7 A. S. Utada, E. Lorenceau, D. R. Link, P. D. Kaplan, H. A. Stone and D. A. Weitz, *Science*, 2005, **308**, 537–541.
8 Z. Nie, W. Li, M. Seo, S. Xu and E. Kumacheva, *J. Am. Chem. Soc.*, 2006, **128**, 9408–9412.
9 D. Saeki, S. Sugiura, T. Kanamori, S. Sato and S. Ichikawa, *Lab Chip*, 2010, **10**, 357–362.
10 D. Conchouso, D. Castro, S. A. Khan and I. G. Foulds, *Lab Chip*, 2014, **14**, 3011–3020.
11 E. Amstad, M. Chemama, M. L. Eggersdorfer, L. R. Arriaga, M. P. Brenner and D. A. Weitz, *Lab Chip*, 2016, **16**, 4163–4172.
12 Y. N. Xia and G. M. Whitesides, *Annu. Rev. Mater. Sci.*, 1998, **28**, 153–184.
13 T. Nisisako and T. Torii, *Lab Chip*, 2008, **8**, 287–293.
14 W. Li, J. Greener, D. Voicu and E. Kumacheva, *Lab Chip*, 2009, **9**, 2715–2721.
15 D. Bardin, M. R. Kendall, P. A. Dayton and A. P. Lee, *Biomicrofluidics*, 2013, **7**, 1–13.
16 T. Nisisako, T. Ando and T. Hatsuzawa, *Lab Chip*, 2012, **12**, 3426–3435.
17 F.-C. Chang and Y.-C. Su, *J. Micromech. Microeng.*, 2008, **18**, 65018.
18 S. Okushima, T. Nisisako, T. Torii and T. Higuchi, *Langmuir*, 2004, **20**, 9905–9908.
19 H. F. Chan, Y. Zhang, Y.-P. Ho, Y.-L. Chiu, Y. Jung and K. W. Leong, *Sci. Rep.*, 2013, **3**, 3462.
20 Y. Zhang, Y.-P. Ho, Y.-L. Chiu, H. F. Chan, B. Chlebina, T. Schuhmann, L. You and K. W. Leong, *Biomaterials*, 2013, **34**, 4564–4572.
21 T. Ward, M. Faivre, M. Abkarian and H. A. Stone, *Electrophoresis*, 2005, **26**, 3716–3724.
22 T. Kawakatsu, Y. Kikuchi and M. Nakajima, *J. Am. Oil Chem. Soc.*, 1997, **74**, 317–321.
23 R. M. Erb, D. Obrist, P. W. Chen, J. Studer and A. R. Studart, *Soft Matter*, 2011, **7**, 8757.
24 S.-H. Kim, J. W. Kim, J.-C. Cho and D. A. Weitz, *Lab Chip*, 2011, **11**, 3162–3166.
25 L. R. Arriaga, E. Amstad and D. A. Weitz, *Lab Chip*, 2015, **15**, 3335–3340.
26 S. Sugiura, M. Nakajima, J. Tong, H. Nabetani and M. Seki, *J. Colloid Interface Sci.*, 2000, **227**, 95–103.
27 I. Kobayashi, M. Nakajima, K. Chun, Y. Kikuchi and H. Fujita, *AIChE J.*, 2002, **48**, 1639–1644.
28 N. Mittal, C. Cohen, J. Bibette and N. Bremond, *Phys. Fluids*, 2014, **26**, 82109.
29 G. Tetradis-Meris, D. Rossetti, C. Pulido de Torres, R. Cao, G. Lian and R. Janes, *Ind. Eng. Chem. Res.*, 2009, **48**, 8881–8889.
30 M. B. Romanowsky, A. R. Abate, A. Rotem, C. Holtze and D. A. Weitz, *Lab Chip*, 2012, **12**, 802–807.
31 G. T. Vladisavljević, N. Khalid, M. A. Neves, T. Kuroiwa, M. Nakajima, K. Uemura, S. Ichikawa and I. Kobayashi, *Adv. Drug Delivery Rev.*, 2013, **65**, 1626–1663.
32 R. Dangla, S. C. Kayi and C. N. Baroud, *Proc. Natl. Acad. Sci. U. S. A.*, 2013, **110**, 853–858.
33 T. Cubaud and T. G. Mason, *Phys. Fluids*, 2008, **20**, 53302.
34 I. Kobayashi, K. Uemura and M. Nakajima, *Colloids Surf., A*, 2007, **296**, 285–289.
35 J. R. Anderson, D. T. Chiu, R. J. Jackman, O. Chemiavskaya, J. C. McDonald, H. Wu, S. H. Whitesides and G. M. Whitesides, *Anal. Chem.*, 2000, **72**, 3158–3164.

